Colloid Polym Sci (2009) 287:395–402
DOI 10.1007/s00396-008-1976-x

ORIGINAL CONTRIBUTION

Aggregation and thermodynamic properties of ionic liquid-type gemini imidazolium surfactants with different spacer length

Mingqi Ao · Peipei Huang · Guiying Xu ·
Xiaodeng Yang · Yajing Wang

Received: 27 August 2008 / Revised: 16 October 2008 / Accepted: 26 November 2008 / Published online: 16 December 2008

Abstract The aggregation behavior and thermodynamic properties of micellization for the ionic liquid-type gemini imidazolium surfactants with different spacer length ([C_{12}–s–C_{12}im]Br_2, s=2, 4, 6) have been investigated by means of surface tension, electrical conductivity, dynamic light scattering and fluorescence measurements. The values of cmc, γ_{cmc}, Γ_{max}, A_{min}, π_{cmc}, pc_{20} and cmc/pc_{20} suggest that the shorter the spacer, the higher the surface activity of [C_{12}–s–C_{12}im]Br_2 is. The cmc and γ_{cmc} values are decreased significantly in the presence of sodium halides, and the values decrease in the order NaCl<NaBr<NaI. The thermodynamic parameters of micellization (ΔG_{m}^0, ΔH_{m}^0, ΔS_{m}^0) indicate that the micellization of [C_{12}–2–C_{12}im]Br_2 and [C_{12}–4–C_{12}im]Br_2 is entropy-driven, whereas aggregation of [C_{12}–6–C_{12}im]Br_2 is enthalpy-driven at lower temperature but entropy-driven at higher temperature. Finally, the fluorescence measurements show that the micropolarity of micelles increases but the aggregation numbers decrease with increasing the spacer length of [C_{12}–s–C_{12}im]Br_2.

Keywords Ionic liquid-type gemini imidazolium surfactant · Spacer length · Adsorption efficiency · Thermodynamics of micellization · Micropolarity

Introduction

Gemini surfactants are thought to have superior properties to those of conventional surfactants, such as lower critical micelle concentrations, better wetting properties, lower limiting surface tensions, higher adsorption efficiency, and so on [1–5]. These surfactants are composed of two hydrophobic chains and two polar head groups covalently attached through a spacer group. Many works have shown that the spacer plays a major role in the aggregation properties of these surfactants [6–13]. Wang et al. [11] have investigated the effect of the nature of spacer on the aggregation properties of cationic gemini surfactants in aqueous solution. They found that the gemini surfactants with a hydrophilic, flexible spacer formed a more closely packed micelle structure than the one with a hydrophobic, rigid spacer. Grosmaire et al. [12] have studied the effect of the spacer carbon number on the enthalpy of micellization for alkanediyl-α,ω-bis(dimethylalkylammonium bromide) surfactants. They found that the ΔH_{m}^0 values were strongly dependent on the spacer carbon number. R. Zana et al. [13] have studied the effect of the spacer group on the association behavior in aqueous solution for gemini quaternary ammonium surfactants. The Cryo-TEM investigations showed that C_{12}–2–C_{12} formed thread-like micelles at a concentration of 2 wt.%. Shorter and still elongated micelles were also visualized in a 7 wt.% solution of C_{12}–3–C_{12}, but the solutions of C_{12}–4–C_{12}, C_{12}–8–C_{12}, and C_{12}–12–C_{12} showed only densely packed spheroidal micelles at 5–7 wt.%.

However, many works about the spacer group mainly focus on the dicationic quaternary ammonium gemini surfactants, the studies of ionic liquid-type gemini imidazolium surfactants with different spacers are so far rare. Ionic liquid-type gemini imidazolium surfactants are a new generation of amphiphilic molecules. Owing to the inherent ionic nature of ionic liquids and the existence of imidazolium head groups, the novel gemini surfactants with different spacer length would have special properties and potential application in many areas, such as skin care, medicine, life science, petrochemistry, textile industry, etc. [14–17]. Therefore, it is significant to study the properties of

---

M. Ao · P. Huang · G. Xu (✉) · X. Yang · Y. Wang
Key Laboratory of Colloid and Interface Chemistry
(Shandong University), Ministry of Education,
Jinan 250100, People's Republic of China
e-mail: xuguiying@sdu.edu.cn

ionic liquid-type gemini surfactants. Previously, we have investigated the surface adsorption and micellization in aqueous solution of three gemini imidazolium surfactants with different hydrophobic chain length ([C_n–4–$C_n$im]Br_2, n=10, 12, 14) which were compared with their corresponding monomers ([$C_n$mim]Br, n=10, 12, 14), and found that the surface activity of [C_n–4–$C_n$im]Br_2 is much higher than that of [$C_n$mim]Br [18]. As an extension of this study, in the present work, a series of ionic liquid-type gemini imidazolium surfactants with the different spacer length ([C_{12}–s–C_{12}im]Br_2, s=2, 4, 6) are synthesized. Their surface activity, thermodynamic properties of micellization and micropolarity of micelle are investigated, and the results show that the spacer length has obvious influence on those properties.

Experimental

Materials

The structures of ionic liquid-type gemini imidazolium surfactants with the different spacer length ([C_{12}–s–C_{12}im]Br_2, s=2, 4, 6) were showed in Fig. 1, which were synthesized in our laboratory. Imidazole, 1,2-dibromoethane, 1,4-dibromobutane, and 1,6-dibromohexane (A.R.) were purchased from Shanghai Reagent Co; 1-Bromododecane (C.P.) was purchased from Alfa-Aesar Reagent Co and used without further purification; and methanol, acrylonitrile, isopropanol, chloroform, acetone were all the analytical grade reagents and were purchased from Tianjin Kemiou Reagent Co. Triply distilled water was used to prepare the solution in all experiments.

Methods

Synthesis of ionic liquid-type gemini imidazolium surfactants

This class of ionic liquid-type gemini imidazolium surfactants was synthesized [19, 20] by mixing 0.15 mol of imidazole and 0.24 mol of acrylonitrile in methanol and stirring for 8 h at 55 °C~60 °C in a nitrogen atmosphere. After that, 0.12 mol of 1-bromodecane was added with isopropanol and the mixture was refluxed at 60 °C~65 °C for 24 h in nitrogen atmosphere. After the reaction finished, the residue was dissolved in chloroform followed by addition of 15 wt.% sodium hydroxide solution and then was stirred at room temperature for 3 h. Subsequently, the chloroform layer was washed several times with deionized water. Residual solvent was removed under vacuum for 2 h at 50 °C. Then, 0.05 mol 1,2-dibromoethane, 1,4-dibromobutane, or 1,6-dibromohexane was added dropwise with isopropanol and the mixture was stirred at 60 °C~65 °C for 24 h in nitrogen atmosphere. After removal of isopropanol, the product was purified five times by recrystallization in acetone and then dried under vacuum for 2 days.

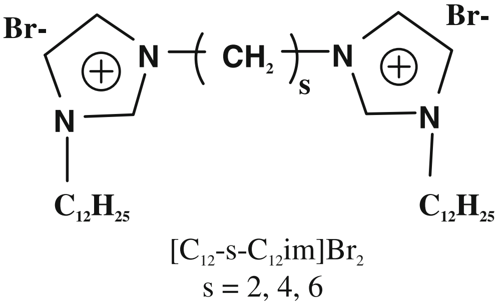

Fig. 1 Chemical structures of ionic liquid-type gemini imidazolium surfactants with different spacer lengths

All the products are characterized by using ^{1}HNMR spectrum (Bruker ADVANCE 400 spectrometer) in $CDCl_3$ and elemental analysis (Vario EI III), and the results are shown below. The results prove that they are all the objective products.

(1) 1,2-bis(3-dodecylimidazolium-1-yl) ethane bromide [C_{12}–2–C_{12}im]Br_2

^{1}HNMR(400MHz, $CDCl_3$): δ(ppm) 10.35(s, 2H), 8.85(s, 2H), 7.16(s, 2H), 5.32(t, 4H), 4.15(t, 4H), 1.92(m, 4H), 1.30(m, 36H), 0.88(t, 6H)

Elemental analysis calculated (%) for $C_{32}H_{60}N_4Br_2$ (660): C 58.18, H 9.09, N 8.48. Found: C 58.29, H 8.96, N 8.48.

(2) 1,4-bis(3-dodecylimidazolium-1-yl) butane bromide [C_{12}–4–C_{12}im]Br_2

^{1}HNMR(400MHz, $CDCl_3$): δ(ppm) 10.35(s, 2H), 7.98(s, 2H), 7.16(s, 2H), 4.60(t, 4H), 4.25(t, 4H), 2.24(m, 4H), 1.91(m, 4H), 1.27(m, 36H), 0.88(t, 6H)

Elemental analysis calculated (%) for $C_{34}H_{64}N_4Br_2$ (688): C 59.30, H 9.30, N 8.14. Found: C 59.21, H 9.32, N 8.07.

(3) 1,6-bis(3-dodecylimidazolium-1-yl) hexane bromide [C_{12}–6–C_{12}im]Br_2

^{1}HNMR(400MHz, $CDCl_3$): δ(ppm) 10.52(s, 2H), 7.94(s, 2H), 7.21(s, 2H), 4.47(t, 4H), 4.29(t, 4H), 2.06(m, 4H), 1.91(m, 4H), 1.52(m, 4H), 1.30(m, 36H), 0.88(t, 6H)

Elemental analysis calculated (%) for $C_{36}H_{68}N_4Br_2$ (716): C 60.34, H 9.50, N 7.82. Found: C 60.21, H 9.45, N 7.68.

The Krafft temperatures of [C_{12}–4–C_{12}im]Br_2 and [C_{12}–6–C_{12}im]Br_2 are all lower than 15 °C. For [C_{12}–2–C_{12}im]Br_2, its solubility is not better than those of [C_{12}–4–C_{12}im]Br_2 and [C_{12}–6–C_{12}im]Br_2, but when its concentration is not higher than 2 mmol/L, it can also keep as a clear aqueous solution at 15 °C. So, in our experimental range, all the experiments can be performed at or above 15 °C.

Surface tension measurement

Surface tension was measured on Processor Tensiometer-K12 (Krüss Company, Germany) using the ring method. Surfactant solutions were kept for 15 min to equilibrate. All the measurements were performed at 25.0±0.1 °C.

Electrical conductivity measurement

Conductivity of the surfactant solutions was measured as a function of concentration with a low-frequency conductivity analyzer (model DDS-307, Shanghai Precision & Scientific Instrument Co., Ltd., accuracy of ±1%) at five different temperatures for each surfactant, and the measurements were repeated twice at each temperature.

Dynamic Light Scattering (DLS)

DLS measurements were carried out using a BI-200SM laser light-scattering spectrometer (Bruker, USA) equipped with a digital correlator (BI-9000AT) at 488 nm. The scattering angle is 90°. All the solutions were prepared by filtering with a 0.2-μm Millipore filter.

Fluorescence measurement

Intensities and spectra of fluorescence were carried out on a Hitachi F-4500 fluorescence spectrophotometer using 1.0-cm quartz cell. Pyrene spectra were recorded with fixed excitation at 335 nm, and the slit widths of excitation and emission were fixed at 2.5 and 10 nm, respectively. The emission spectra were scanned over the spectra range of 350–550 nm. Intensities, I_1 and I_3, were taken from the emission intensities at 373 and 384 nm and then the ratio of I_1/I_3 was used to estimate the micropolarity sensed by pyrene as well as to obtain the cmc of the surfactants in aqueous solution at 25 °C. The pyrene concentration was fixed at 1.0×10^{-6} mol/L in all the measurements.

The micelle aggregation number, N_{agg}, can be calculated according to the equation [21]:

$$\ln\left(\frac{I_0}{I}\right) = \frac{N_{\mathrm{agg}}C_{\mathrm{Q}}}{C_{\mathrm{s}} - \mathrm{cmc}} \tag{1}$$

where I_0 and I are the fluorescence intensities of pyrene in the absence and presence of the quencher (benzophenone) at a specific wavelength of 273 nm, C_{Q} and C_{s} are the molar concentration of the quencher and the surfactants, respectively. The pyrene concentration was fixed at 1.0×10^{-6} mol/L.

Results and discussion

Surface activity of ionic liquid-type gemini surfactants with different spacer length

The surface tension measurement is a classical method to study the surface activity of surfactants. The surface tension isotherms of $[\mathrm{C}_{12}\text{–}s\text{–}\mathrm{C}_{12}\mathrm{im}]\mathrm{Br}_2$ are shown in Fig. 2. All of them show a sharp break in the surface tension isotherm, which are the indicative of the critical micelle concentration (cmc) and the formation of micelles. It is worth mentioning that the absence of a minimum around the breakpoint confirms that there are no higher active substances in these ionic liquid-type surfactants. The surface activity parameters of $[\mathrm{C}_{12}\text{–}s\text{–}\mathrm{C}_{12}\mathrm{im}]\mathrm{Br}_2$ are listed in Table 1. As can be seen, the shorter spacer length, the lower cmc and γ_{cmc} values are. This result demonstrates that the surface activity of $[\mathrm{C}_{12}\text{–}s\text{–}\mathrm{C}_{12}\mathrm{im}]\mathrm{Br}_2$ with shorter spacer length is higher than that with longer spacer length.

The packing densities of surfactants at the air/aqueous solution interface are also important for the interpretation of surface activity of the various materials. The A_{min} occupied by the surfactant at the air/aqueous interface should reflect their packing densities. The saturation adsorption values Γ_{max} at the air/aqueous interface are calculated using the following Gibbs adsorption isotherm equation:

$$\Gamma_{\mathrm{max}} = -\frac{1}{nRT}\times\frac{d\gamma}{d\,l\,nc} \tag{2}$$

where γ is the surface tension in mN/m, Γ_{max} is the saturation adsorbed amount in μmol/m^2, R is the gas constant (8.314 J mol^{-1} K^{-1}), T is the absolute temperature, c is the surfactant concentration, and ($\mathrm{d}\gamma/\mathrm{d}lnc$) is the slope in the surface tension isotherm when the concentration is

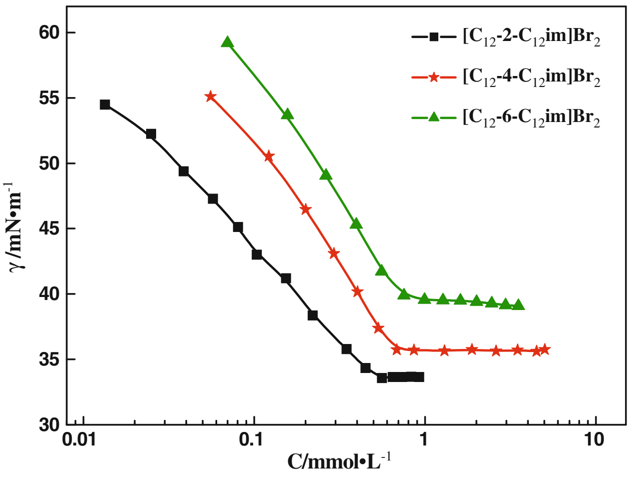

Fig. 2 Surface tension isotherms of $[\mathrm{C}_{12}\text{–}s\text{–}\mathrm{C}_{12}\mathrm{im}]\mathrm{Br}_2$ surfactants. The error of surface tension value is ±0.2 mN/m

near the cmc. The value of n is taken as 3. Then the $A_{\min}$ can be obtained from the saturated adsorption:

$$A_{\min} = (N_A \Gamma_{\max})^{-1} \times 10^{24} \tag{3}$$

where N_A is Avogadro's number and $A_{\min}$ is in nm^2. Both the $\Gamma_{\max}$ and $A_{\min}$ values are listed in Table 1. It is seen that $A_{\min}$ values are 1.35, 1.40, 1.43 nm^2 for [C_{12}–2–C_{12}im]Br_2, [C_{12}–4–C_{12}im]Br_2, [C_{12}–6–C_{12}im]Br_2, respectively. The increase of $A_{\min}$ values with increasing spacer length suggests that [C_{12}–2–C_{12}im]Br_2 has higher packing density at the air/aqueous solution interface than those of [C_{12}–4–C_{12}im]Br_2 and [C_{12}–6–C_{12}im]Br_2. A possible explanation is that the hydrophilic head groups with the shorter spacer can pack more tightly at the interface and thus make the $A_{\min}$ value smaller.

From the surface tension plots, two additional parameters can be obtained, i.e., the adsorption efficiency, pc_{20}, and the effectiveness of surface tension reduction, π_{cmc}. The former parameter is defined as [22]:

$$pc_{20} = -\log c_{20} \tag{4}$$

where c_{20} is the surfactant concentration at which the surface tension of pure solvent is reduced by 20 mN/m. It is the minimum concentration needed to lead to a saturation of the surface adsorption. Thus, pc_{20} can be measured the efficiency of adsorption of surfactant at the air/aqueous interface. The larger value of pc_{20}, the higher adsorption efficiency of the surfactant is. The other parameter, π_{cmc}, is the surface pressure at the cmc, being defined by Eq. (5):

$$\pi_{\mathrm{cmc}} = \gamma_0 - \gamma_{\mathrm{cmc}} \tag{5}$$

where γ_0 and γ_{cmc} are the surface tensions of pure solvent and the solution at cmc, respectively. This parameter indicates the maximum reduction of surface tension caused by the dissolution of surfactant molecules, hence, it becomes a measure for the effectiveness of the surfactant to lower the surface tension of the solvent [22], and the greater the π_{cmc} value, the higher the effectiveness of surfactant is. The values of these two parameters are listed in Table 1. It can be seen that both pc_{20} and π_{cmc} values increase in the order [C_{12}–6–C_{12}im]Br_2<[C_{12}–4–C_{12}im]Br_2<[C_{12}–2–C_{12}im]Br_2, which indicates that [C_{12}–2–C_{12}im]Br_2 is superior to the another two surfactants in both the adsorption efficiency (pc_{20}) and the effectiveness of surface tension reduction (π_{cmc}).

Table 1 Surface properties of the ionic liquid-type gemini imidazolium surfactants [C_{12}–s–C_{12}im]Br_2

Surfactants	[C_{12}–2–C_{12}im] Br_2	[C_{12}–4–C_{12}im] Br_2	[C_{12}–6–C_{12}im] Br_2
cmc/mmol L^{-1}	0.55	0.72	0.78
γ_{cmc}/mN m^{-1}	33.6	35.7	39.5
$\Gamma_{\max}$	1.23	1.19	1.16
$A_{\min}$	1.35	1.40	1.43
π_{cmc}/mN m^{-1}	38.4	36.3	32.5
pc_{20}	4.54	3.94	3.73
cmc/c_{20}	18.97	6.32	4.13

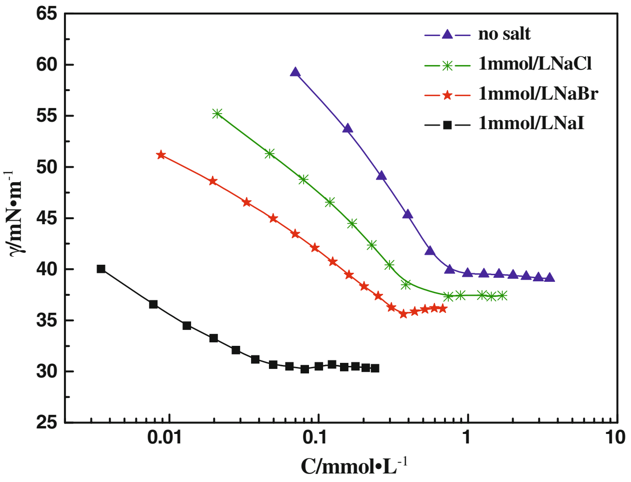

Fig. 3 Surface tension as a function of concentration of [C_{12}–6–C_{12}im]Br_2 in the absence or presence of 1 mmol/L sodium halides

A convenient way of measuring the relative effects of some structural or microenvironment factor on micellization and on adsorption is to determine its effect on the cmc/c_{20} ratio [22]. The cmc/c_{20} ratio affords insights into the adsorption and micellization processes. The surfactant with larger cmc/c_{20} ratio has the greater tendency to adsorb at the interface, compared with its tendency to form micelles. The values of cmc/c_{20} are 18.97, 6.32 and 4.13 for [C_{12}–2–C_{12}im]Br_2, [C_{12}–4–C_{12}im]Br_2 and [C_{12}–6–C_{12}im]Br_2, respectively. Obviously, they decrease with increasing the spacer length, suggesting that in comparison with micellization, the adsorption at the air/aqueous interface for [C_{12}–s–C_{12}im]Br_2 with shorter spacer length is easier.

Effect of sodium halides on the surface activity of gemini imidazolium surfactants

The surface tension of aqueous solution of these gemini imidazolium surfactants was measured in the presence of NaCl, NaBr and NaI. As a representative example, Fig. 3 shows the results obtained for [C_{12}–6–C_{12}im]Br_2. The surface tension as well as the cmc of [C_{12}–6–C_{12}im]Br_2 is reduced by all the sodium halides. The cmc and γ_{cmc} values of these gemini imidazolium surfactants in the presence of NaCl, NaBr and NaI are summarized in Table 2. The decrease in the cmc and γ_{cmc} values caused by the salt addition may be interpreted as follows. The cationic surfactant forms ionic monolayer at the air/water interface, the addition of electrolyte anions leads to the reduction of the thickness and potential of the electric double layer at the interface because of the electrostatic interaction between opposite charges [23]. Consequently, it induces the screening of the electrostatic repulsion among the polar head groups and leads to remarkably lower cmc and γ_{cmc} in comparison with the salt-free system. Summarized from Table 2 and taking the values of cmc in the presence of 1.0 mmol/L NaBr as an example, the cmc decrease about 77.3%, 62.5%, and 60.6%, for $[C_{12}–2–C_{12}im]Br_2$, $[C_{12}–4–C_{12}im]Br_2$ and $[C_{12}–6–C_{12}im]Br_2$, respectively. Namely, the salt effect decreases in the order $[C_{12}–2–C_{12}im]Br_2 > [C_{12}–4–C_{12}im]Br_2 > [C_{12}–6–C_{12}im]Br_2$. This is because the surfactants with shorter spacer have the stronger electrostatic repulsion among the polar head groups. Once the sodium halide is added, the electrostatic repulsion can be screened immediately due to the electrostatic interaction between opposite charges, and this effect is more remarkable for the surfactants with shorter spacer length which would behave the stronger salt effect. Meanwhile, it is seen from Fig. 3, the sodium halides at the same concentration lower the cmc and γ_{cmc} values of $[C_{12}–6–C_{12}im]Br_2$ in the order NaCl<NaBr<NaI. It is because the ion, being more polarizable, is easier to penetrate into the surface layer and more effective in neutralizing the charges of cationic head groups in the monolayer. The strongly polarized halide anions like Br^- or I^- seem to be more "surface active" than weakly polarized ones (Cl^-). They have the tendency to accumulate in the surface layer due to strong interaction with the electric field at the interface and this tendency increases in the order $Cl^- < Br^- < I^-$ [23]. So, the influence of NaI is the most obvious.

Degree of counterion binding to micelles (β)

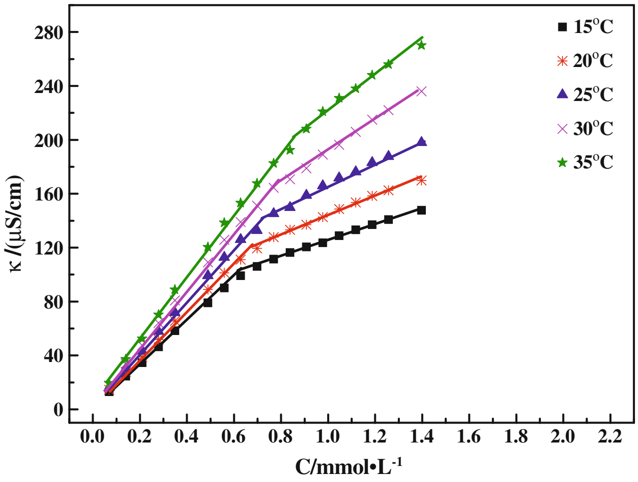

Fig. 4 The plots of electrical conductivity, κ, against concentration of $[C_{12}–6–C_{12}im]Br_2$ at different temperatures. The error of electrical conductivity value is ±0.2 μS/cm

A comprehension of the specific binding of counterions to micelles is a prerequisite for an understanding of micellization and of all kinds of aggregation in aqueous solutions [24]. So, the electrical conductivity measurements are used to study the aggregation behavior of $[C_{12}–s–C_{12}im]Br_2$ in aqueous solutions. Taking $[C_{12}–6–C_{12}im]Br_2$ as an example, the changes of the κ as a function of concentration are shown in Fig. 4 at five temperatures. As can be seen that the plot of the conductivity, κ, versus the concentration, c, in the aqueous phase is linear, with a break at the cmc, above which the (decreased) slope of the plot again becomes linear. The break in the plot is a result of the reduction in the effective charge on the micelles, due to the binding of some counterions to the micelles above the cmc. The cmc of $[C_{12}–s–C_{12}im]Br_2$ surfactants estimated from electrical conductivity plots at different temperatures are listed in Table 3. It may be seen that the cmc increases upon raising the temperature, and by and large, the values of cmc measured from electrical conductivity at 25 °C are in agreement with those obtained from surface tension. The degree of counterion dissociation, α, can be obtained from the ratio of the slopes above and below the cmc, while the degree of counterion binding to micelle, β, is $(1-\alpha)$. The β values at various temperatures are also listed in Table 3. It is reported [25, 26] that the degree of counterion binding to micelle, β, is dependent on the size of micelles. The larger micelle has a greater tendency to attract counterions than the smaller one, means it has the stronger ability of counterion binding to micelles, i.e., the larger β value. As can be clearly seen from Table 3, the β values of $[C_{12}–s–C_{12}im]Br_2$ surfactants all decrease with the increase of temperature. So, we can speculate that the micelle of $[C_{12}–s–C_{12}im]Br_2$ surfactants would be smaller in size at higher temperature than at lower temperature which can be

Table 2 cmc and γ_{cmc} of $[C_{12}–s–C_{12}im]Br_2$ in the presence of sodium halides

Salt	Concentration (mmol/L)	$[C_{12}–2–C_{12}im]Br_2$		$[C_{12}–4–C_{12}im]Br_2$		$[C_{12}–6–C_{12}im]Br_2$	
		cmc (mmol/L)	γ_{cmc} (mN m^{-1})	cmc (mmol/L)	γ_{cmc} (mN m^{-1})	cmc (mmol/L)	γ_{cmc} (mN m^{-1})
NaCl	1.0	0.470	32.9	0.608	35.3	0.707	37.3
NaBr	1.0	0.125	30.5	0.270	33.9	0.307	36.2
NaI	1.0	0.028	28.6	0.043	30.1	0.050	31.0

Table 3 Effect of spacer length and temperature on parameters of micellization for $[C_{12}–s–C_{12}im]Br_2$ surfactants

Surfactant	Temperature °C	cmc mmol/L	β	ΔG_m^0 kJ/mol	ΔH_m^0 kJ/mol	$T\Delta S_m^0$ kJ/mol
$[C_{12}–2–C_{12}im]Br_2$	15	0.59	0.83	−34.87	−7.16	27.71
	20	0.62	0.81	−34.76	−6.23	28.53
	25	0.64	0.77	−34.41	−5.21	29.20
	30	0.66	0.74	−33.75	−4.13	29.62
	35	0.67	0.69	−33.05	−3.04	30.01
$[C_{12}–4–C_{12}im]Br_2$	15	0.68	0.75	−33.85	−5.44	28.41
	20	0.71	0.72	−33.48	−5.58	27.90
	25	0.73	0.70	−33.41	−5.77	27.64
	30	0.76	0.65	−32.44	−5.80	26.64
	35	0.79	0.60	−31.43	−5.82	25.61
$[C_{12}–6–C_{12}im]Br_2$	15	0.61	0.63	−30.89	−18.14	12.75
	20	0.67	0.61	−30.62	−17.02	13.60
	25	0.74	0.60	−30.59	−15.98	14.61
	30	0.80	0.57	−30.04	−14.60	15.44
	35	0.86	0.55	−29.77	−13.32	16.45

confirmed by dynamic light scattering (DLS). Such as $[C_{12}–6–C_{12}im]Br_2$, the apparent hydrodynamics radius decrease from 4.0 nm at 25 °C to 2.5 nm at 35 °C as seen in Fig. 5.

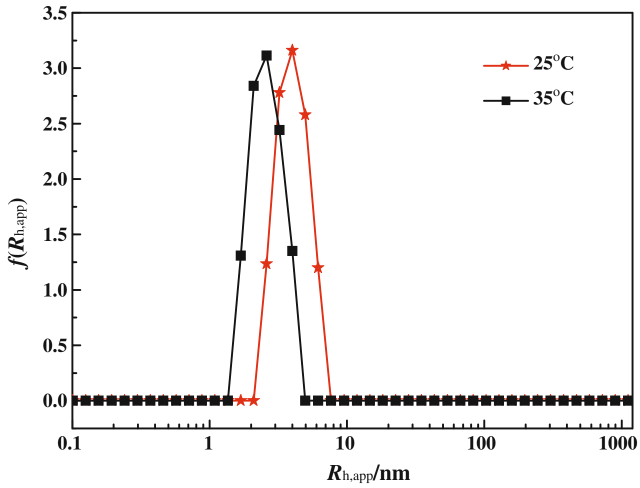

Fig. 5 Apparent hydrodynamic radius ($R_{h,app}$) of $[C_{12}–6–C_{12}im]Br_2$ micelles formed in the aqueous solution at the concentration of 2 mmol/L at 25 °C and 35 °C, respectively

Thermodynamic parameters

The phase separation model is applied to compute the thermodynamic parameters of micellization, and the standard Gibbs free energy change of micellization can be calculated from the following equation [27]:

$$\Delta G_m^0 = RT(0.5 + \beta)\ln X_{cmc} \tag{6}$$

where X_{cmc} is the cmc in molar fraction, which X_{cmc}=cmc/55.4, cmc is that in mol/L, and 55.4 comes from that 1 L of water corresponds to 55.4 mol of water at 25 °C. β is the degree of counterion binding to micelles. The standard enthalpy change for the micellization process, ΔH_m^0, can be determined using the Gibbs–Helmholtz equation for aqueous solutions:

$$\left[\frac{\partial\left(\Delta G_m^0/T\right)}{\partial(1/T)}\right] = \Delta H_m^0 \tag{7}$$

$$\Delta H_m^0 = -RT^2(0.5 + \beta)\ln X_{cmc}/d\,T \tag{8}$$

Then, the standard entropy of micelle formation, ΔS_m^0, is obtained by the use of the following relation:

$$\Delta S_m^0 = \left(\Delta H_m^0 - \Delta G_m^0\right)/T \tag{9}$$

The thermodynamic parameters of micellization at different temperatures for $[C_{12}–s–C_{12}im]Br_2$ are listed in Table 3. As can be seen, the standard Gibbs free energy changes with different spacer length are all negative, indicating that the formation of micelle is spontaneous. The values of standard enthalpy changes (ΔH_m^0) for micellization are negative as well, implying the micelle formation process is exothermic. The ΔH_m^0 values do not vary significantly upon raising the temperature, this can be understood when it is assumed that London dispersion interactions represent the main attractive force for micelle formation [28]. Of course, they also indicate no significant variation in the environment surrounding the hydrophobic chain of the surfactant molecule with temperature variation. The data of $[C_{12}–2–C_{12}im]Br_2$ and $[C_{12}–4–C_{12}im]Br_2$ in Table 3 indicate that the negative values of ΔG_m^0 are mainly due to the large positive of ΔS_m^0. ΔH_m^0 is much smaller than the value of $T\Delta S_m^0$, therefore, the micellization process is governed primarily by the entropy gain associated with it,

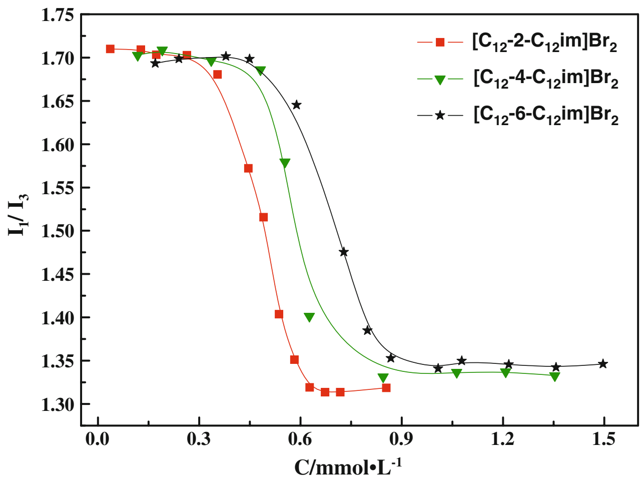

Fig. 6 I_1/I_3 ratio of pyrene as a function of concentration for [C$_{12}$–s–C$_{12}$im]Br$_2$ in aqueous solution

namely the micellization is entropy-driven, and the driving force for the process is the tendency of the hydrophobic group of the surfactant to transfer from the solvent environment to the interior of the micelle. However, for [C$_{12}$–6–C$_{12}$im]Br$_2$, the variation is different. The $\Delta H_{\mathrm{m}}^{0}$ values of [C$_{12}$–6–C$_{12}$im]Br$_2$ increase upon raising the temperature, while $(-T\Delta S_{\mathrm{m}}^{0})$ values decrease with increasing the temperature, and $(-T\Delta S_{m}^{0})$ intersects with $\Delta H_{\mathrm{m}}^{0}$ in the range 25–30 °C. This indicates that an enthalpy term plays the dominant role to negative $\Delta G_{\mathrm{m}}^{0}$ below ~25 °C, while the contribution of an entropy term $(-T\Delta S_{\mathrm{m}}^{0})$ becomes dominant above ~25 °C. In other words, the micelle formation process of [C$_{12}$–6–C$_{12}$im]Br$_2$ is enthalpy-driven at lower temperature, while entropy-driven at higher temperature. At lower temperature, the enthalpy-driven is probably due to the longer spacer which may increase the degree of hydration of the hydrophilic head groups in micellization. But at higher temperature, because the structure of water bound by the spacer and the hydrophobic chains are destroyed, and the freedom of the hydrophobic chain in the nonpolar interior of the micelle increase, resulting in the contribution of $\Delta S_{\mathrm{m}}^{0}$ to $\Delta G_{\mathrm{m}}^{0}$ increasing and larger than that of $\Delta H_{\mathrm{m}}^{0}$.

Microenviroment and aggregation number of micelle

The micellization for [C$_{12}$–s–C$_{12}$im]Br$_2$ was also investigated by steady-state fluorescence using the emission of pyrene. Pyrene monomer fluorescence emission is useful for monitoring the self-aggregation in aqueous solution. Because the fluorescence intensities for various vibronic bands in the pyrene monomer fluorescence show strong polarity dependence, pyrene exhibits a characteristic fluorescence emission spectrum consisting of five bands in the region of 370–400 nm. In polar media, the 0–0 band (peak1) for pyrene molecules is enhanced by a mechanism involving vibronic coupling similar to the Ham effect in the adsorption spectra of benzene [29]. Thus, the intensity ratio of the first to the third vibronic peaks, i.e., I_1/I_3, is often used as a measure of the polarity of the microenvironment [30]. When surfactant self-assembly takes place, pyrene molecules will penetrate into the interior hydrophobic region of micelles from water. This will cause an abrupt change of the I_1/I_3 ratio and the concentration corresponding to this abrupt change is the cmc. Figure 6 represents the I_1/I_3 ratio variation with the surfactant concentration, the cmc values taken at the inflection point are 0.59, 0.72, and 0.80 mmol/L for [C$_{12}$–2–C$_{12}$im]Br$_2$, [C$_{12}$–4–C$_{12}$im]Br$_2$ and [C$_{12}$–6–C$_{12}$im]Br$_2$, respectively, which are in accordance with those obtained from surface tension and electrical conductivity measurements. As seen in Fig. 6, above the cmc, the I_1/I_3 values are independent of each surfactants concentration and they are 1.31, 1.33, and 1.34 for [C$_{12}$–2–C$_{12}$im]Br$_2$, [C$_{12}$–4–C$_{12}$im]Br$_2$, and [C$_{12}$–6–C$_{12}$im]Br$_2$, respectively. These low I_1/I_3 values indicate that pyrene is solubilized in the palisade layer near the polar head groups for all the gemini surfactant micelles [31]. The I_1/I_3 values above the cmc decrease following the order [C$_{12}$–2–C$_{12}$im]Br$_2$<[C$_{12}$–4–C$_{12}$im]Br$_2$<[C$_{12}$–6–C$_{12}$im]Br$_2$, the length of spacer in the hydrophilic head group may be responsible for this result. Because of the longer spacer, the hydrophilic head groups can not be closer with each other than those with shorter spacer. This would result in a less tightly packing of the palisade layer, and lead more water molecules to exist in the palisade layer of the gemini surfactant micelles, consequently, leading pyrene molecules to sense more polar microenvironment, and then, having the larger I_1/I_3 values.

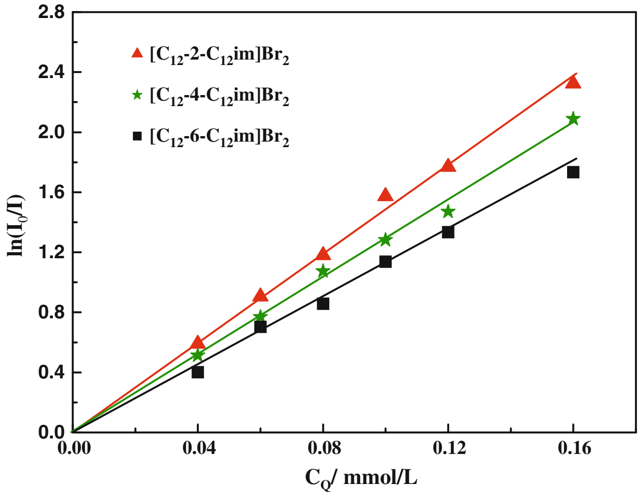

Fig. 7 $\ln(I_0/I)$ of pyrene as a function of concentration of the quencher benzophenone in the [C$_{12}$–s–C$_{12}$im]Br$_2$ aqueous solutions

Figure 7 shows the relationship between C_Q and $\ln(I_0/I)$ for $[C_{12}$–*s*–$C_{12}im]Br_2$ surfactants. The concentrations of the surfactants used are all 2.0 mmol/L. The plots give straight lines in all the cases. The values of N_{agg} obtained from the slope of each straight line and they are found to be 21, 16, and 14 for $[C_{12}$–2–$C_{12}im]Br_2$, $[C_{12}$–4–$C_{12}im]Br_2$ and $[C_{12}$–6–$C_{12}im]Br_2$, respectively. Results show that the aggregation number decreases upon increasing the spacer length. The reason may be that the longer spacer remains in extended conformation and allows it to aggregate relatively loose to form smaller aggregates. This result is corresponding to that of micropolarity of micelle.

Conclusions

In this work, ionic liquid-type gemini imidazolium surfactants with different spacer length $[C_{12}$–*s*–$C_{12}im]Br_2$ (*s*=2, 4, 6) have been synthesized and their surface activity, thermodynamic properties of micellization and micropolarity of micelles have been studied. It is concluded from the data of cmc, γ_{cmc}, Γ_{max}, A_{min}, π_{cmc}, pc_{20}, and cmc/c_{20} ratio that the surface activity of $[C_{12}$–2–$C_{12}im]Br_2$ is higher than those of $[C_{12}$–4–$C_{12}im]Br_2$ and $[C_{12}$–6–$C_{12}im]Br_2$. The effects of sodium halides, NaCl, NaBr, and NaI, on micellization are also studied by surface tension measurements. The cmc and γ_{cmc} values are decreased significantly in the presence of sodium halides, and the values decrease in the order NaCl<NaBr<NaI. The thermodynamic parameters of micellization $\left(\Delta G_m^0, \Delta H_m^0, \Delta S_m^0\right)$ derived from electrical conductivity demonstrate that the micellization process of $[C_{12}$–2–$C_{12}im]Br_2$ and $[C_{12}$–4–$C_{12}im]Br_2$ is the entropy-driven process, while that of $[C_{12}$–6–$C_{12}im]Br_2$ is enthalpy-driven at lower temperature and entropy-driven at higher temperature. Finally, the fluorescence measurements suggest that the micropolarity of micelles increases but the aggregation numbers decrease with increasing the spacer length of $[C_{12}$–*s*–$C_{12}im]Br_2$.

Acknowledgment The authors are grateful to the Natural Science Foundation of Shandong Province, China (Y2007B32).

References

1. Zana R (2002) Adv Colloid Interface Sci 97:205–253
2. Menger FM, Keiper JS (2000) Angew Chem Int Ed 39:1906–1920
3. Kim SS, Zhang WZ, Pinnavaia TJ (1998) Science 282:1302–1305
4. Bernd T (2005) Colloid Polym Sci 283:421–430
5. Bell PC, Bergsma M, Dolbnya IP et al (2003) J Am Chem Soc 125:1551–1558
6. De S, Aswal VK, Goyal PS, Bhattacharya S (1998) J Phys Chem B 102:6152–6160
7. Rosen MJ, Mathias JH, Davenport L (1999) Langmuir 15:7340–7346
8. Wettig SD, Verrall RE (2001) J Colloid Interface Sci 235:310–316
9. Wettig SD, Nowak P, Verrall RE (2002) Langmuir 18:5354–5359
10. Mathias JH, Rosen MJ, Davenport L (2001) Langmuir 17:6148–6154
11. Wang XY, Wang JB, Wang YL, Yan HK (2004) Langmuir 20:53–56
12. Grosmaire L, Chorro M, Chorro C et al (2002) J Colloid Interface Sci 246:175–181
13. Zana R (2002) J Colloid Interface Sci 248:203–220
14. Badea I, Wettig S, Verrall R, Foldvari M (2007) Eur J Pharm Biopharm 65:414–422
15. Yang H, Shen ZW, Zhou XJ (2005) Langmuir 21:10931–10940
16. André L, Klaus L, Rivo HR, Laurent W (2005) Colloid Polym Sci 283:469–479
17. Tae-Soo C, Yoshio S, Hirofusa S, Kunihiro H (2001) Dyes Pigments 50:55–65
18. Ao MQ, Xu GY, Zhu YY, Bai Y (2008) J Colloid Interface Sci 326:490–495
19. Baltazar QQ, Chandawalla J, Anderson JL (2007) Colloids Surf A 302:150–156
20. Ding YX, Zha M, Zhang J, Wang SS (2007) Colloids Surf A 298:201–205
21. Turro NJ, Yekta A (1978) J Am Chem Soc 100:5951–5952
22. Rosen MJ (2004) Surfactants and interfacial phenomena, 3rd edn. Wiley, New York, p p 83,149,215
23. Para G, Jarek E, Warszynski P (2006) Adv Colloid Interface Sci 122:39–55
24. Moroi Y (1992) Micelles: theoretical and applied aspects. Plenum, New York, p 61
25. Bhattacharya S, Haldar J (2004) Langmuir 20:7940–7947
26. Tsao HK (1998) J Phys Chem B 102:10243–10247
27. Zana R (1996) Langmuir 12:1208–1211
28. Nusselder JJH, Engberts JBFN (1992) J Colloid Interface Sci 148:353–361
29. Koyanagi M (1968) J Mol Spectrosc 25:273–290
30. Zana R, Levy IHM, Duportail G (1997) Langmuir 13:5552–5557
31. Kalyanasundaram K, Thomas JK (1997) J Am Chem Soc 99:2039–2044